

Observation of the First Excited State in ^{23}O

N. Frank^{1,2,3}, A. Schiller¹, T. Baumann¹, D. Bazin¹, J. Brown⁴,
P. A. DeYoung⁵, J. E. Finck⁶, A. Gade¹, J. Hinnefeld⁷, R. Howes⁸,
J.-L. Lecouey^{1,a}, B. Luther³, W. A. Peters^{1,2}, H. Scheit¹, and
M. Thoennessen^{1,2}

¹ National Superconducting Cyclotron Laboratory,
Michigan State University, East Lansing, MI 48824

² Department of Physics & Astronomy,
Michigan State University, East Lansing, MI 48824

³ Department of Physics, Concordia College, Moorhead, MN 56562

⁴ Department of Physics, Wabash College, Crawfordsville, IN 47933

⁵ Department of Physics, Hope College, Holland, MI 49423

⁶ Department of Physics, Central Michigan University, Mt. Pleasant, MI 48859

⁷ Department of Physics & Astronomy,
Indiana University at South Bend, South Bend, IN 46634

⁸ Department of Physics, Marquette University, Milwaukee, WI 53201

Abstract. The first excited state in neutron-rich ^{23}O was observed in a (2p1n) knock-out reaction from ^{26}Ne on a beryllium target at a beam energy of 86 MeV/A. The state is unbound with respect to neutron emission and was reconstructed from the invariant mass from the ^{22}O fragment and the neutron. It is unbound by 45(2) keV corresponding to an excitation energy of 2.8(1) MeV. The non-observation of further resonances implies a predominantly direct reaction mechanism of the employed three-nucleon-removal reaction which suggests the assignment of the observed resonance to be the $5/2^+$ hole state.

Keywords: Invariant mass method, neutron-rich nuclei, direct reaction, knock-out reactions

PACS: 21.10.Pc, 23.90.+w, 25.60.Gc, 29.30.Hs

1. Introduction

It has been established that the traditional magic numbers can disappear for nuclei far from stability [1, 2]. At the same time rearrangement of single particle orbits opens new gaps leading to new magic numbers [3]. In order to search for and study these changes, several observables have to be measured, for example, binding energies and the level structure of excited states. For very neutron-rich nuclei close to the neutron dripline none or only a few bound excited states exist, and for nuclei beyond the dripline even the ground state is unbound with respect to neutron emission. Thus, γ -ray spectroscopy is not feasible and other detection methods have to be utilized. In very light nuclei these states can be populated with multiple-particle transfer reactions from stable beams [4, 5]. Another method is β -delayed neutron spectroscopy where neutron-unbound excited states are populated via β -decay from neutron-rich isotopes produced in fast fragmentation reactions [6, 7]. However, some nuclei can only be studied with the method of neutron-decay spectroscopy, where the states of interest are populated either directly by fast fragmentation reactions [8, 9, 10], or by few nucleon knockout reaction of secondary beams (which first were produced by fast fragmentation) [11, 12]. The excited states are then reconstructed from the invariant mass of the emitted neutron and coincident fragment.

Figure 1 shows the region of light, neutron-rich isotopes of the nuclear chart. Stable and neutron-bound isotopes are shown as black and dark grey squares, respectively. Unbound nuclei beyond the dripline where some spectroscopy information is available and which have merely been determined to be unbound are shown

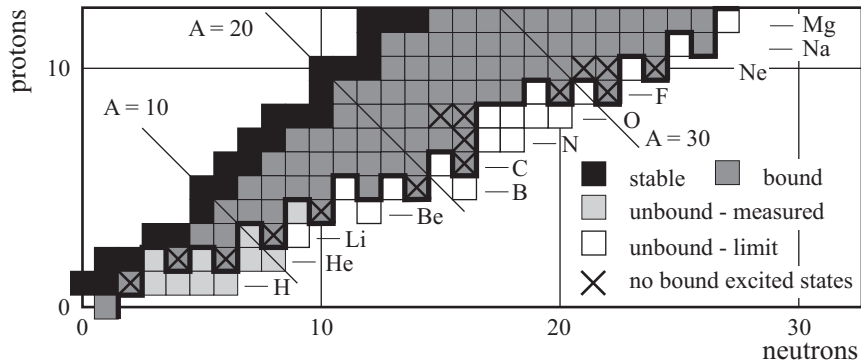


Fig. 1. Section of the chart of nuclei. Stable and neutron-bound isotopes are shown as black and dark grey squares, respectively. Unbound nuclei beyond the dripline where some spectroscopy information is available and which have merely been determined to be unbound are shown as light grey and white squares, respectively. Nuclei with no bound excited states are indicated by crosses.

as light grey and white squares, respectively. Nuclei with no bound excited states are indicated by crosses. Of these states only ^{23}O and ^{31}Ne are accessible with β -delayed neutron spectroscopy.

In neutron-rich oxygen isotopes, the magic number $N = 20$ has vanished and new gaps at $N = 14$ and $N = 16$ have appeared [13, 14]. No bound excited states have been observed in ^{23}O or ^{24}O [15] which is the last bound oxygen isotope [16, 17, 18]. ^{23}O is especially interesting because it is located between the new shell gaps. While single particle states probe the $N = 16$ shell gap, single hole states probe the $N = 14$ gap. The present study searches for the first excited state of ^{23}O using the method of neutron decay spectroscopy and the selective (2p1n) knockout reaction from ^{26}Ne .

2. Experimental Set-up

The experiment was performed at the National Superconducting Cyclotron Laboratory at Michigan State University. A 105 pA primary beam of 140 MeV/A ^{40}Ar impinged on a 893 mg/cm² Be production target. The resulting cocktail beam was purified with respect to the desired ^{26}Ne at 86 MeV/A using an achromatic 750-mg/cm²-thick acrylic wedge degrader in the A1900 fragment separator [19]. A purity of up to 93.2% was achieved with a ^{26}Ne beam intensity of about 7000 pps. The contaminants (mainly ^{27}Na and ^{29}Mg) were separated event-by-event in the off-line analysis by their different time-of-flight (ToF) from the extended focal plane to a scintillator in front of the 721-mg/cm²-thick Be reaction target. Positions and angles of incoming beam particles were measured by two 15×15 cm² position-sensitive parallel-plate avalanche counters (PPACs) with ~ 8 pads/cm, i.e., FWHM ≈ 1.3 mm. The presence of a quadrupole triplet downstream of the PPACs translates this into a position resolution of impinging ^{26}Ne particles on the target within a FWHM radius of 2.4 mm.

Charged particles behind the target were bent 43° by the large-gap 4 Tm Sweeper Magnet [20]. Two 30×30 cm² cathode-readout drift chambers (CRDCs) provided position in the dispersive (~ 4 pads/cm, FWHM ≈ 2.5 mm) and non-dispersive (drift time, FWHM ≈ 3.1 mm) direction. The 1.87 m distance between the CRDCs translates this into FWHM = 2.4 mrad angle resolution. Energy loss was determined in a 65-cm-long ion chamber (IC) and a 40×40 cm², 4.5-mm-thin plastic scintillator whose pulse-height signal was corrected for position. Energy loss was used to separate reaction products with different Z . The thin scintillator also gave ToF of reaction products from the target. This, together with the total kinetic energy measurement in a 15-cm-thick plastic scintillator, provided isotopic separation. Further details can be found in [21, 22].

Beam-velocity neutrons were detected in the Modular Neutron Array (MoNA) [23, 24] at a distance of 8.2 m from the target with an intrinsic efficiency of $\sim 70\%$. MoNA consists of 9×16 stacked 2-m-long plastic scintillator bars which are read out on both ends by photomultiplier tubes (PMT). The bars are mounted horizontally

and perpendicular to the beam axis. Position along the vertical and along the beam axis is determined within the thickness of one bar (10 cm). Horizontal position and neutron ToF are determined by the time difference and the mean time, respectively, of the two PMT signals which yield resolutions of $\text{FWHM} \approx 12$ cm and $\text{FWHM} \approx 0.24$ ns, see also [22, 25].

The decay energies of resonances are reconstructed by the invariant mass method. To do this, the relativistic four-momentum vectors of the neutron and fragment are reconstructed at the point of breakup. For neutrons, position and ToF resolution translate into angle and energy resolution of $\text{FWHM} = 19$ mrad and $\text{FWHM} = 3.8$ MeV, respectively. The angle and energy of fragments in coincidence with neutrons were reconstructed behind the target based on the ion-optical properties of the Sweeper Magnet using a novel method which takes into account the position at the target in the dispersive direction [26]. The reconstructed position in the non-dispersive direction serves thereby as a check on an event-by-event basis against the same information obtained from forward tracking from the PPACs through the quadrupole triplet. The angle and energy resolution of the fragments behind the target are $\text{FWHM} = 6.4$ mrad and $\text{FWHM} = 0.9$ MeV/ A , respectively. The average energy loss of the fragment through half of the target is added to approximate the relativistic four-momentum vector of the fragment at the average breakup point.

3. Results

Figure 2 shows the decay energy spectrum for ^{23}O reconstructed from neutrons in coincidence with ^{22}O fragments. The data were compared with simulations based on a Glauber reaction model including angle straggling of the fragments in the target as well as detector resolutions. The data in the figure are best described by a Breit-Wigner resonance contribution (dashed curve) with $E_r = 45(2)$ keV and an energy-independent single-particle width of $\Gamma \sim 0.1$ keV plus a contribution from a beam-velocity source of Maxwellian-distributed neutrons (a thermal model) with $T \sim 0.7$ MeV (dash-dotted curve). The decay-energy resolution is dominated by the neutron-angle resolution and contributions due to the target thickness. The thermal model has been included in the fit as a phenomenological description for non-resonant contribution to the spectrum.

The decay energy (45(2) keV) of the resonance can be related to an excitation energy (2.79(13) MeV) by adding the neutron-separation energy $S_n = 2.74(13)$ MeV of ^{23}O [29] under the assumption that the decay populates the ground state of ^{22}O . The other alternative, that this decay proceeds via an excited state in ^{22}O is unlikely because the first excited state in ^{22}O is located at an excitation energy of 3.2 MeV. It would place the narrow resonance at an excitation energy of 6 MeV in ^{23}O and it would be hard to reconcile the absence of any low energy unbound states in the spectrum.

The observation of only one resonance in the decay-energy spectrum can be ex-

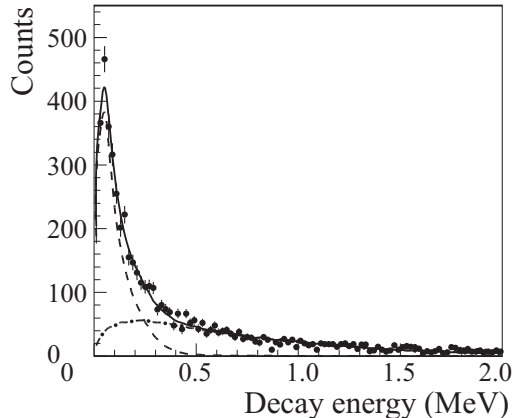


Fig. 2. Decay-energy spectra of $^{23}\text{O}^*$ (data points). The thick solid curve corresponds to the sum of the dashed (simulated resonant contribution) and dash-dotted (simulated thermal model) curves and agrees well with the data.

plained because the most straightforward reaction mechanism directly determines the spin assignment of the state. The ground-state wave function of the secondary beam of ^{26}Ne has large spectroscopic overlap with the $1/2^+$ ground state of ^{23}O (a $\nu(1s_{1/2})^{-1}$ hole state) [27] and the $5/2^+$ excited state, but the cross section for this three-nucleon knockout reaction is rather small. A more likely scenario is the two-proton knockout involving one valence $\pi(0d_{5/2})$ and one core $\pi(0p)$ proton. (The knockout of both valence protons ($\pi(0d_{5/2})^2$) will simply populate the ^{24}O ground state.) These excitations decay via negative-parity neutron-excitation admixtures as shown in Figure 3. The proton configuration ($\pi(0p) + \pi(0d_{5/2})^{-1}$) shown on the left mixes with (from left to right) neutron excitations of the form $\nu(0p)^{-1} \times \nu(0d_{3/2})^1$, $\nu(1s_{1/2})^{-1} \times \nu(0f1p)^1$, and $\nu(0d_{5/2})^{-1} \times \nu(0f1p)^1$. The first of which has large spectroscopic overlap with high-lying negative-parity excitations in ^{23}O ; the other two will excite one neutron (either a $1s_{1/2}$ or a $0d_{5/2}$) to the continuum of the fp -shell. The current setup is not efficient for the detection of these high-energy neutrons which probably contribute to the non-resonant background described above. The resulting ^{23}O is then in the $1/2^+$ ground state and the $5/2^+$ excited state, respectively. The subsequent neutron decay of the $5/2^+$ state is the resonance observed in our experiment. Although it is not possible to distinguish between the three-nucleon knockout and the two-proton knockout followed by neutron-emission, neither mechanism populates the $3/2^+$ (particle) excited state. It should be mentioned that this state has recently been observed for the first time in the single-neutron transfer reaction $^{22}\text{O}(d,p)^{23}\text{O}^*$ [28].

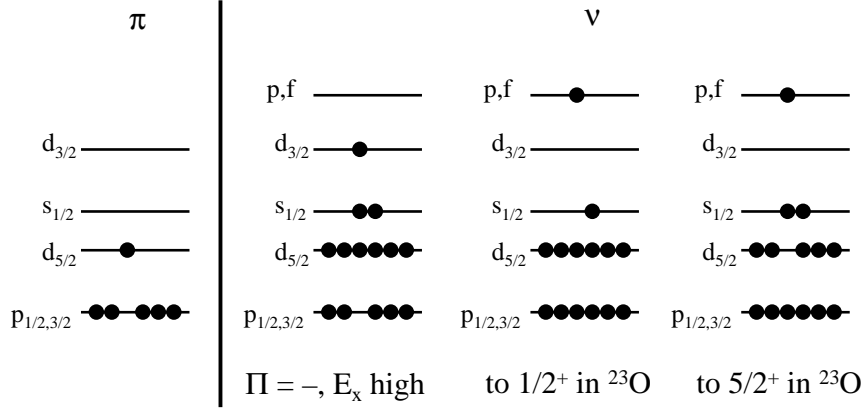


Fig. 3. Admixture of proton excitations and neutron excitations. The left side shows the knockout of the core (p -shell) proton. The neutron level diagrams on the right show three possible scenarios for cross shell neutron excitations; see text for explanation.

4. Conclusions

In conclusion, we have observed a 45(2) keV resonance in the n - ^{22}O decay-energy spectrum which we interpret as the $5/2^+$ first excited state of ^{23}O . The observation is consistent and complementary with the recent observation of the $3/2^+$ state by Elekes *et al.* [28]. The non-observation of any higher-lying resonances implies selectivity of the relevant reaction mechanism: either a direct three-nucleon removal or a core plus valence two-proton removal followed by neutron emission.

Acknowledgments

We would like to thank the members of the MoNA collaboration G. Christian, C. Hoffman, K.L. Jones, K.W. Kemper, P. Pancella, G. Peaslee, W. Rogers, S. Tabor, and about 50 undergraduate students for their contributions to this work. We would like to thank R.A. Kryger, C. Simenel, J.R. Terry, and K. Yoneda for their valuable help during the experiment. Financial support from the National Science Foundation under grant numbers PHY-01-10253, PHY-03-54920, PHY-05-55366, PHY-05-55445, and PHY-06-06007 is gratefully acknowledged. J.E.F. acknowledges support from the Research Excellence Fund of Michigan.

Note

- a.* Permanent address: Laboratoire de Physique Corpusculaire, ENSICAEN, IN2P3, 14050 Caen, Cedex, France

References

1. A. Navin *et al.*, Phys. Rev. Lett. **85**, 266 (2000).
2. Zs. Dombardi *et al.*, Phys. Rev. Lett. **96**, 182501 (2006).
3. B.A. Brown, Prog. Part. Nucl. Phys. **47**, 517 (2001).
4. R. Kalpakchieva *et al.*, Eur. Phys. J. A **7**, 451 (2000).
5. G. Bohlen *et al.*, Eur. Phys. J. A **31**, 279 (2007).
6. C.S. Sumithrarachchi, D.W. Anthony, P.A. Lofy, D.J. Morrissey, Phys. Rev. C **74**, 024322 (2006).
7. C.S. Sumithrarachchi *et al.*, Phys. Rev. C **75**, 024305 (2007).
8. F. Deák *et al.*, Nucl. Instrum. Methods Phys. Res. **A258**, 67 (1987)
9. R.A. Kryger *et al.*, Phys. Rev. C **47**, R2439 (1993).
10. M. Thoennessen *et al.*, Phys. Rev. C **59**, 111 (1999).
11. M. Zinser *et al.*, Nucl. Phys. **A619**, 151 (1997).
12. L. Chen, B. Blank, B.A. Brown, M. Chartier, A. Galonsky, P.G. Hansen, M. Thoennessen, Phys. Lett. **B 505**, 21 (2001).
13. A. Ozawa, T. Kobayashi, T. Suzuki, K. Yoshida, and I. Tanihata, Phys. Rev. Lett. **84**, 5493 (2000).
14. P.G. Thirolf *et al.*, Phys. Lett. **B 485**, 16 (2000).
15. M. Stanoiu *et al.*, Phys. Rev. C **69**, 034312 (2004).
16. M. Langevin *et al.*, Phys. Lett. **B 150**, 71 (1985).
17. D. Guillemaud-Mueller *et al.*, Phys. Rev. C **41**, 937 (1990).
18. O. Tarasov *et al.*, Phys. Lett. **B 409**, 64 (1997).
19. D.J. Morrissey, B.M. Sherrill, M. Steiner, A. Stolz, and I. Wiedenhoever, Nucl. Instrum. Methods Phys. Res. **B204**, 90 (2003).
20. M.D. Bird *et al.*, IEEE Trans. Appl. Supercond. **15**, 1252 (2005).
21. N. Frank, Ph.D. thesis, Michigan State University, 2006.
22. A. Schiller *et al.*, *subm. for publ.* (2007).
23. B. Luther *et al.*, Nucl. Instrum. Methods Phys. Res. **A505**, 33 (2003)
24. T. Baumann *et al.*, , Nucl. Instrum. Methods Phys. Res. **A543**, 517 (2005).
25. W.A. Peters, Ph.D. thesis, Michigan State University, 2007.
26. N. Frank *et al.*, *subm. to Nucl. Instrum. Methods Phys. Res. A*, (2007)
27. J.R. Terry *et al.*, Phys. Lett. **B 640**, 86 (2006).
28. Z. Elekes *et al.*, Phys. Rev. Lett. **98**, 102502 (2007).
29. G. Audi, A.H. Wapstra, and C. Thibault, Nucl. Phys. **A729**, 337 (2003).